Arch. Metall. Mater. **66** (2021), 4, 1187-1193

DOI: 10.24425/amm.2021.139437

M. SOLECKA[1]*, B. RUTKOWSKI[2], A. KOPIA[2]

KINETICS OF THE HIGH TEMPERATURE OXIDATION OF THE INCONEL 686 COATINGS IN THE WASTE INCINERATION ASH

In this paper, detailed characterization of the oxide scale, grown on the Inconel 686 coating after high-temperature oxidation at 650°C in ashes from waste incineration power plant was performed. Phase composition, morphology, microstructure and chemical composition of the oxide scale were investigated using XRD and SEM analysis. Mechanisms of formation and growth of oxide scales were examined, resulting in the insights into oxidation kinetics. Results revealed presence of NiO in the outermost layer of the oxide scale. At the bottom of oxide scale, $CrNi_2O_4$ spinel layers were formed due to the increasing concentration of Cr. In the middle area of oxide scale, due to higher concentration of Cr and lower amount of Ni, the Cr_2NiO_4 spinel is formed. The innermost layer was composed of Cr_2O_3.

Keywords: Inconel 686 alloy; SEM; XRD; High-temperature corrosion

Introduction

Among wide range of Ni-based superalloys, Inconel 686 is an advanced corrosion resistant material. Due to its high performance in aggressive environments it is widely used in several industrial sectors, including petrochemical, air pollution control and power generation systems [1,2]. Inconel 686 is available in all standard produced forms, including: plate, sheet, pipe, tube, rod, bar, forging stock, and matching composition welding products [3] and mainly contains nickel, chromium, molybdenum and tungsten. Carbon content is restricted to 0.01%, what facilitates in diminishing precipitation at the grain boundaries in the heat-effected zone (HAZ) of welded areas to uphold the corrosion resistance [3]. Generally, good corrosion resistance of Ni-Cr-Mo alloys is assured due to the formation of adherent, dense and thermodynamically stable oxide scales, based on NiO and Cr_2O_3 components. Sims [4] showed that 15-20 wt% Cr content in Ni-base alloys assures reasonable degree of protection against high temperature oxidation, whereas above 18% of chromium is needed to form continuous chromium scale [5].

Corrosion process is even more destructive if the reaction of the corrosion products with an ash (originating from combustion of biomass), wastes and heavy oil occurs. Such inexpedient reactions with ash present at the surface of oxide scale, containing dangerous oxides, sulphides and chlorides lead to formation of aggressive low melt eutectic [6-8]. These products may again react with components of the combustion gases. In this way a complex series of interacting heterogeneous reactions takes place. The ash layer shows differences in chemical composition, and it is related to the temperature gradient. The mechanism resulting from the corrosive ash components interaction is extremely complex and depends not only on chemical composition of ash but it depends also on the reaction conditions and type of substrate exposed to the corrosive environments [5,8,9].

The oxidation mechanism of metal at the high temperature under the ash atmosphere usually depends on the oxygen transport from ashes to the bulk material of alloy as a result of diffusion of alloy cations to the alloy/ash interface [10]. The oxidation of metal at the high-temperature conditions should be considered as electrochemical process. Therefore, in the case of Inconel alloys, the process of oxide layer formation at the surface of the clean metal starts with the adsorption of oxygen by Ni and Cr atoms, according to the chemical reactions (Eq. (1 and 2)):

$$2Ni + O_2 – (g) \rightarrow 2NiO\ (s) \quad (1)$$

$$4\ Cr + 3\ O_2\ (g) \rightarrow 2Cr_2O_3\ (s) \quad (2)$$

[1] INSTITUTE OF METALLURGY AND MATERIALS SCIENCE, POLISH ACADEMY OF SCIENCES, 25 REYMONTA STR., 30-059 KRAKOW, POLAND
[2] AGH UNIVERSITY OF SCIENCE AND TECHNOLOGY, FACULTY OF METALS ENGINEERING AND INDUSTRIAL COMPUTER SCIENCE, AL. A. MICKIEWICZA 30, 30-059 KRAKÓW, POLAND

* Corresponding author: solecka.monika@gmail.com; m.solecka@imim.pl

Many authors have investigated the diffusion of chromium and oxygen in Cr_2O_3 and most of them have found that chromium diffusion was faster than oxygen diffusion [11-14].

The Cr_2O_3 particles were surrounded with NiO and the solid-state reaction occurs to form spinel according to the chemical reaction (Eq. (3)):

$$Cr_2O_3 + NiO \rightarrow Cr_2NiO_4\ (s) \quad (3)$$

Moreover, the Cr_2NiO_4 spinel can also reduce the diffusion rate of metal ion, what decreases the bonding rate of the metal and oxygen ions [15], therefore the oxidation resistance of the alloys will be enhanced. The growth kinetics of these oxides, at steady-state conditions fulfill a parabolic law, what is in agreement with Wagner's oxidation theory [16].

Among a variety of welding techniques, cladding is another form of surface treatment, where the surface of bulk material is protected by the layer of another, corrosion resistant, material. The clad layer has more superior properties than those of the bulk material. Chemical composition of the clad layer should be homogenous and the concentration of Fe entering from the base material into the coating should be as low as possible. To produce Ni-based weld overlays without introducing too much Fe, a new, automatic weld technique called Cold Metal Transfer (CMT) was used [17]. The protection against corrosion is assured with Ni-based superalloys, most commonly Inconel 625 or Inconel 686. The steel tubes are cladded circumferentially in protective gas shroud. Cladding material is supplied in form of wire, which is melted due to current flow. A uniform layer is formed in one pass. In the clad layer the welding incompatibilities such as pores and discontinuities may appear but using the CMT method significantly reduces the occurrence of these imperfections. The following investigations are very important due to limited information about corrosion resistance of the Inconel 686, whereas many studies focus on investigating the corrosion resistance of Inconel 625 [18-22].

In the present study the high temperature oxidation behavior of Inconel 686 alloy at 650°C for 100, 1000 and 2000 hours was investigated. Oxide scale morphology, its chemical composition at the surface and through cross–section were studied with various diffraction and microscopic techniques. The growth and formation mechanisms of oxide scales were examined, giving the insights into oxidation kinetics.

1. Materials and methods

The external surface of 16Mo3 steel boiler tube was clad with Inconel 686 alloy by the CMT method in the SEFAKO S.A. boiler factory (Fig. 1a). The chemical composition of the investigated Inconel 686 clad layer, 16Mo3 steel and the ashes, sampled from a fluidized bed waste incinerator is shown in Table 1.

In the CMT process, the wire is moved towards the work piece (boiler tube) until a short circuit occurs. Flowing by the wire current causes it to melt. After certain time, circuit is automatically opened due to the wire retraction. Now, the wire moves towards the work piece once again and the process reiterate. The general parameters of the cladding process are given in Table 2.

Samples for experiments have form of 15 mm × 10 mm × 1.5 mm coupons (Fig. 1b). The outer surface of specimen

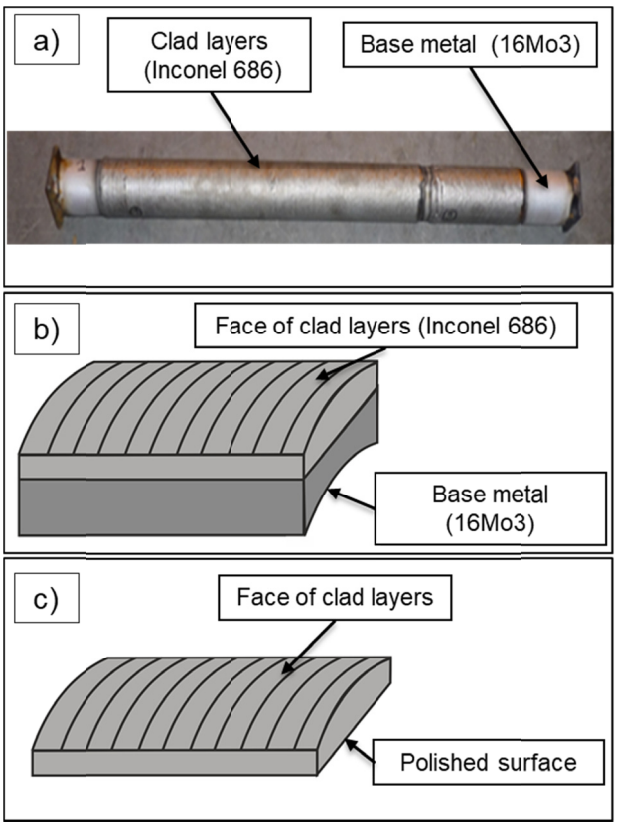

Fig. 1. a) Schematic diagram of Inconel 686 clad layers on the boiler tube; b) piece cut out from clad tube; c) specimen with removed base metal, ready for corrosion experiments in ashes

TABLE 1

Chemical composition of: Inconel 686 wires used for cladding, 16 Mo3 boiler tubes substrate and ashes (%, wt.)

Element	Concentrations (wt., %)		
	Inconel 686	16Mo3	Ashes
Nickel	balance	—	—
Chromium	19.0-23.0	max. 0.3	—
Molybdenum	15.0-17.0	max. 0.3	—
Tungsten	3.0-4.0	—	—
Iron	max. 2.0	balance	2.5
Manganese	max. 0.75	max. 0.65	—
Silicon	max. 0.08	max. 0.35	22
Titanium	0.02-0.25	—	—
Cobalt	max. 1.0	—	—
Phosphorus	max. 0.04	—	—
Calcium	—	—	37.7
Oxygen	—	—	23.5
Chlorygen	—	—	2
Sodium	—	—	1.5
Aluminium		—	3
Sulfur	—	—	3
Carbon	max. 0.01	max. 0.16	5

TABLE 2

CMT cladding parameters

Clad rod	Cladding current (A)	Cladding voltage (V)	Gas flow rate (litre/min)	Feed speed rate (metre/min)	Peripheral speed rate (rotation/min)
Inconel 625	200	20	17	0.8	4.5

consists of Inconel 686 layer deposited on the surface of 16Mo3 steel boiler tube. Before oxidation, the 16Mo3 base material was completely removed by grinding with abrasive paper. Polishing on diamond suspensions was used in order to obtain mirror – like surface on the substrate side (Fig. 1c). Polished and cleaned in ethanol Inconel 686 clad layer samples were placed in a ceramic crucible. Subsequently, they were covered with around 1 cm thick layer of the waste incinerations ashes and exposed to temperature of 650°C for 100 to 2000 h (Fig. 2a). The overview of the Inconel 686 clad layer before oxidation is presented in Fig. 2b, whereas Inconel 686 clad layer samples after oxidation in waste incineration ashes for 100, 1000 and 2000 hours are shown in Figures 2c-e respectively. The oxidation products were studied by X-ray diffraction technique (XRD) using PANanalytical Empyrean DY 1061 diffractometer with filtered Cu Kα $\lambda = 1.54060$ Å radiation at 40 kV and 40 mA. The X-ray diffraction measurement were made with Bragg-Brentano geometry in the 2θ range of 20-80 degree. The step size and the time per step were fixed to 0.05° and 10 s, respectively. The X-ray diffraction spectra were recorded with PANalytical HighScore Plus software. The surface morphology and chemical composition of oxidized Inconel 686 clad layer were investigated with the use of scanning electron microscopy (SEM) Inspect 550, FEI company, equipped with energy dispersive spectrometer (EDS) by EDAX.

Subsequently, the samples were sputtered with thin layer of Au. Afterwards, Ni-coating was deposited electrochemically to protect the oxide scales against damage during metallographic preparation. Metallographic cross-sections were then prepared by standard grinding procedures, as described by Solecka et al. [23]. The SiO suspension with a particle size approx. 0.05 μm was used for final polishing.

2. Results and discussion

The microstructure and characteristics of Inconel 686 alloy clad layer have been examined and discussed elsewhere [22,24-26]. These studies have shown presence of (Nb, Ti)C in the clad layers matrix of γ phase. Moreover, precipitates of other phases (Laves, P and σ) were observed [22,25]. Chemical composition analysis revealed the microsegregtion of Mo, Cr and Fe into the cellular-dendritic microstructure of Inconel 686 clad layers. The Fe content is clearly higher in the partially mixed zone than in the fusion zones and decreases with the distance from the interface (fusion boundary) towards the coating surface [22,24-26].

In following study, above described coating was exposed to waste incineration ashes at 650°C for 100, 1000 and 2000 h. As a result of corrosion products formation, oxidized samples

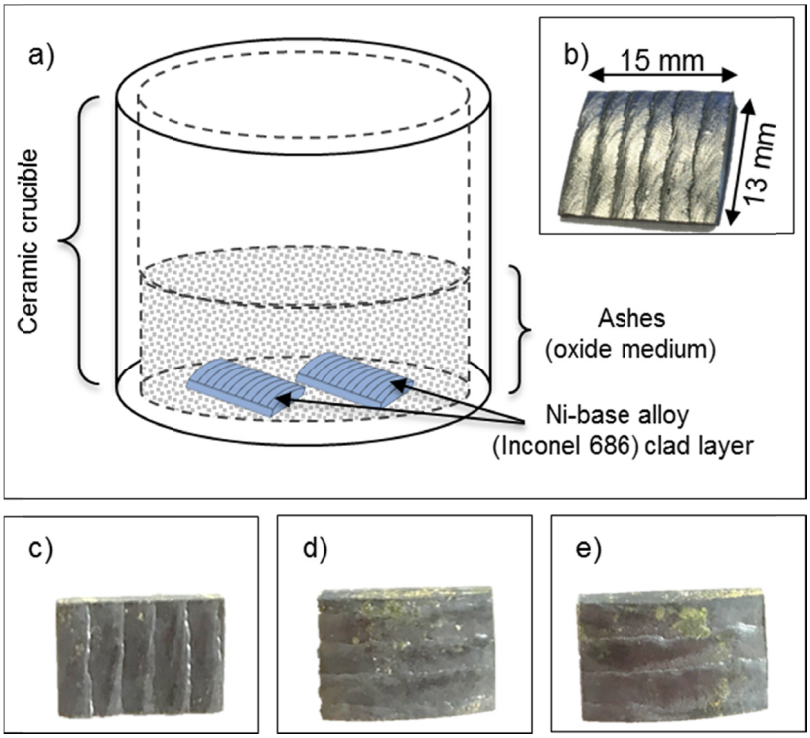

Fig. 2. Schematic of the corrosion experiments in ashes at 650°C (a), and b) the Inconel 686 clad layer before oxidation; (c,d,e) Inconel 686 clad layer after oxidation for 100, 1000 and 2000 h, respectively

lost their metallic lustre (Fig. 2b), acquiring a grey color with locally occurring bright green areas (Fig. 2c-e), representing ash residues on the surface of the clad layer.

According to Mrowec [5] as well as Young [11], the first stages of oxidation might be controlled by the phase boundary reaction, therefore oxidation kinetics shall be linear. After some time of the oxidation, when the oxide scale will be thickened, the diffusion will start to control the oxidation process. Therefore the oxidation may proceed according to the parabolic oxidation kinetics [5,11]. In the other words, corrosion process is slowing down with the extension of the superalloy oxidation time. As the oxidation time increases, a continuous scale forms on the surface of clad layers, which separates the superalloy from the oxidizing environment. Further scale growth is therefore difficult because inward oxygen diffusion and outward metal diffusion is hindered. The inner layer is adherent to clad surface and is consisted of metal oxides with a lower degree of oxidation and a lower oxygen concentration. The recrystallization of oxide scale after gaining thickness as well as significant volatility of the oxide scale at elevated temperatures might be a reason of the outer porous layer formation [5,11].

The Bragg-Brentano X-ray diffraction spectrum for Inconel 686 samples after corrosion test for 100, 1000 and 2000 h are presented in Figure 3. The strongest peaks at 2θ angle of 45.6 and 50.5° corresponding to Inconel 686 substrate (g). The corrosion scale is composed of three main components – Cr_2O_3, Cr_2NiO_4 and NiO. Strong peaks corresponding to NiO (analysis of NiO phase was made base on diffraction pattern no. 04-006-7439) are visible at 2θ angle of 37.3, 43.3, 62.9, 75.4 and 79.4° what is consistent with literature data [28]. Peaks corresponding to Cr_2O_3 are visible at 2θ angle of around 24.4, 33.5, 41.5 and 54.5°, whereas peaks at 2θ angle of around 36, 57, 62.9 and 74.5° corresponding to Cr_2NiO_4 spinel. Increase intensity of NiO peaks (at 2θ angle of 37.3, 62.9 and 79.4°) and Cr_2NiO_4 peaks (at 2θ angle of 36, 57, 62.9) after 1000 h of oxidation time indicates

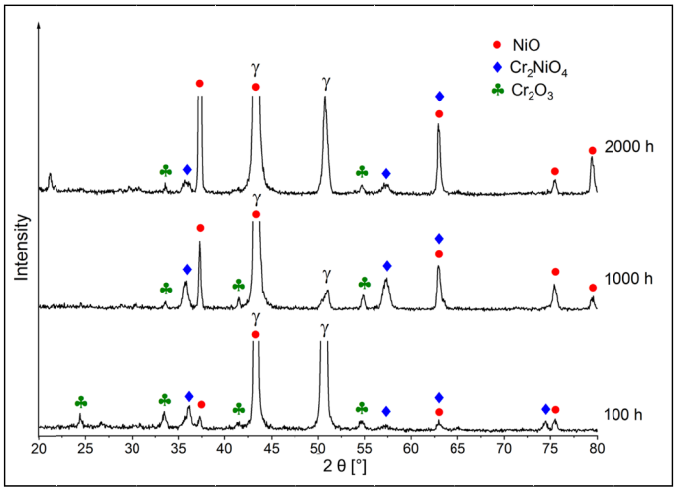

Fig. 3. XRD Bragg-Brentano pattern of the Inconel 686 clad layer after oxidation in waste incineration ashes for 100, 1000 and 2000 h at 650°C

the increasing thickness of the oxidized layer by growth of NiO and Cr_2NiO_4. Reduction of the peaks intensity of Cr_2NiO_4 and Cr_2O_3 after 2000 h suggesting NiO as the top layer of corrosion products.

Further analysis were performed on the cross-sections. Scanning electron microscopy allows for qualitative analysis of oxides. The morphology of the scale formed on the outer side of the Inconel 686 clad layer is shown in Fig. 4a. Observations made on the surface revealed the presence of oxide scale with homogeneous morphology. Some sharp-edged polyhedral crystals are occurring (Fig. 4a), suggesting that coarse grained nickel oxide (NiO) is formed on the entire outer surface. The presence of NiO has been confirmed by XRD analysis (Fig. 3). The morphology of the sample cross-section was presented in Fig. 4b.

The long-term corrosion process was evaluated through the measurement of the scale thickness increase, as shown in Fig. 5. Usually, the mass measurements performed during the corrosion

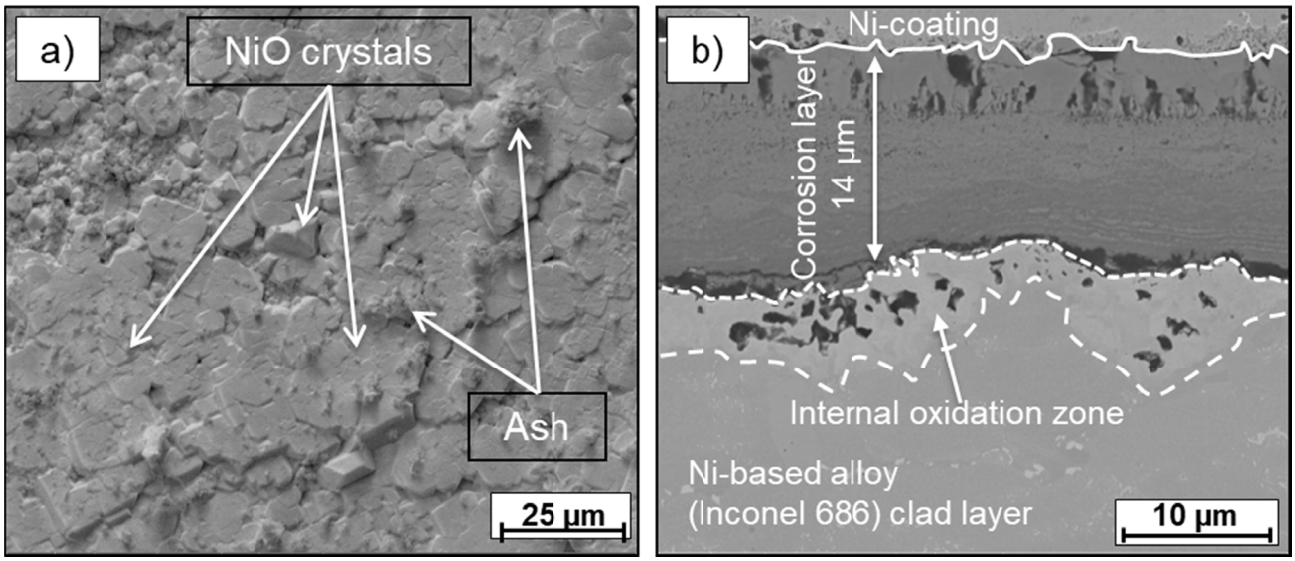

Fig. 4. Morphology and microstructure of the Inconel 686 clad layer after exposure at 650°C in ashes for 2000 h: a) surface (plan view), SEM-SE; b) cross-section, SEM-BSE

process are used as an input data for the oxidation kinetics. In the case of corrosion tests in the ash environment, however, mass measurement may be erroneous, mainly due to presence of the residuals of ash on the surface, disturbing in the correct measurement. The thickness of the oxide scales was measured with scanning electron microscopy on the cross-sections of the samples after oxidation in the ashes at 650°C for 100, 250, 500, 1000 and 2000 h. For each sample, the thickness measurement was carried out on a distance of 1 mm. Every value in the diagram (Fig. 5) is the average of 100 measurements. The standard deviation is also indicated. It is worth to mention that oxide scale is multilayered, however, the overall thickness of all layers was measured. It is also explicit that the thickness of the formed layer increases with the oxidation time. After 100 h of oxidation in the ashes, the average thickness of the oxide scale formed on the surface was 3.95 (±1.10) mm, whereas after 1000 h the average thickness increased to 10.10 (±2.23) mm and after 2000 h thickness increased to 12.15 (±2.60) mm (Fig. 5). Note that oxide scales after longer time of exposition (1000, 2000 h) had very non-uniform thickness. In the latter case, the thinnest region had a thickness of 10 um, whereas the 25 um was found for its thickest part (Fig. 5). On the basis performed investigations, it might be concluded that oxide layer thickness increase kinetics has a parabolic form. It is further supported by the results of the microstructural observations. The corrosion process of the investigated superalloy is relatively fast at the beginning and getting slower with the oxidation time.

Fig. 6 presents the results of EDS chemical composition mapping, which graphically show the cross sectional distributions of the Ni, Cr and O in Inconel 686 clad layer after exposure at 650°C in ashes for 100, 1000 and 2000 h, respectively. Performed microstructural investigations reveal that the oxide scales are characterized by the significant thickness variation and porosity. Elemental maps of Ni, Cr and O showing non-uniform, multi-layered structure, which is clearly visible in Figure 6c. Moreover, these layers are intertwined with each other. After 1000 h of oxidation, under the oxide scale the Cr depleted zone still contains some amount of Cr, which is able to form Cr_2O_3 oxide. After 2000 h of oxidation, the interface between the oxide scale and the base metal is very irregular. Moreover, the base metal right under the oxide scale is drained out of Cr on the thickness of ~5 um. It might have serious implication during further oxidation. Since no Cr is present, the Ni will oxidize next. According to analysis of cross-section and XRD results (Fig. 3), it could be assumed that NiO is formed at the outermost layer in contact with the waste incineration ashes, whereas Cr_2NiO_4 and Cr_2O_3 are located more internally, near the Inconel 686 alloy substrate.

In addition, the higher Ni concentration in Inconel 686 alloy promoted the formation of NiO. Chevalier et al. [29] found that the Ni at the NiO grain boundaries has 1-2 orders of magnitude higher thermal diffusion coefficient of oxygen when the environment temperature is less than 800°C. NiO is mainly formed by the diffusion of Ni to the alloy surface via the grain boundaries

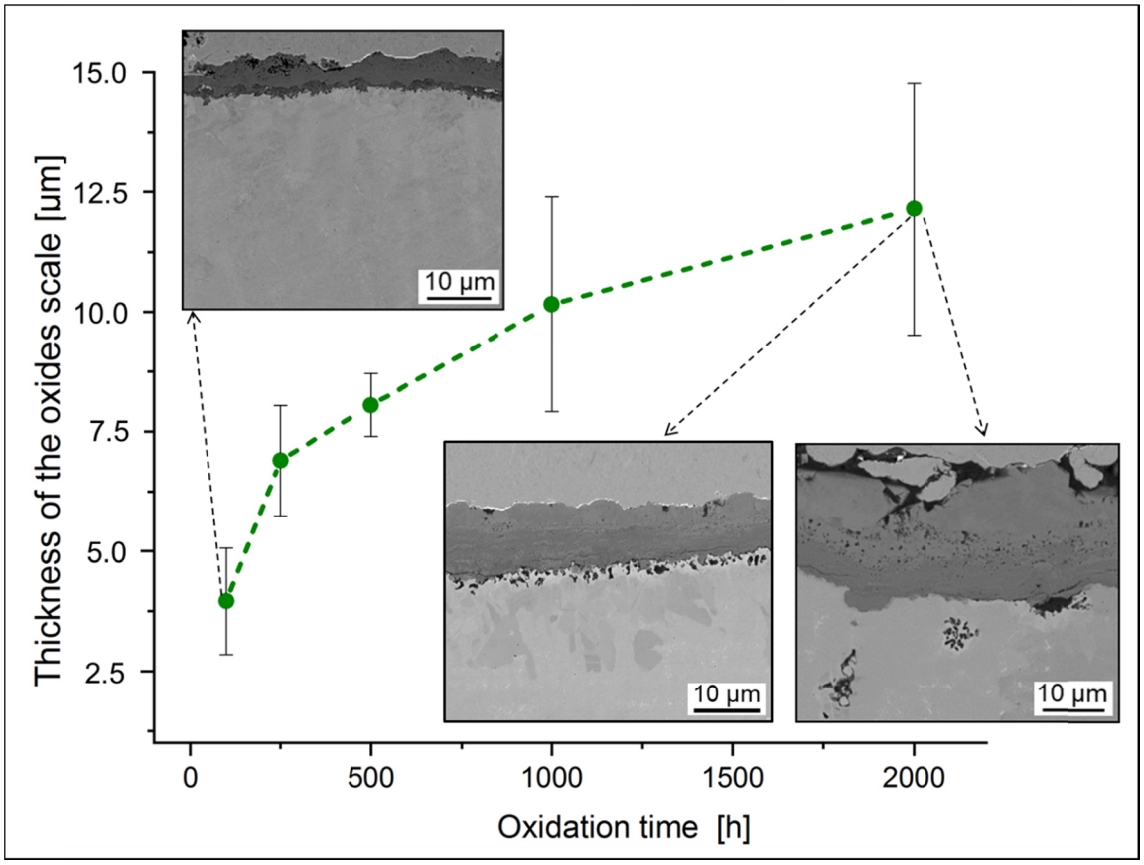

Fig. 5. Thickness of the oxide scale grown on Inconel 686 clad layer after exposure at 650°C after different times of oxidation

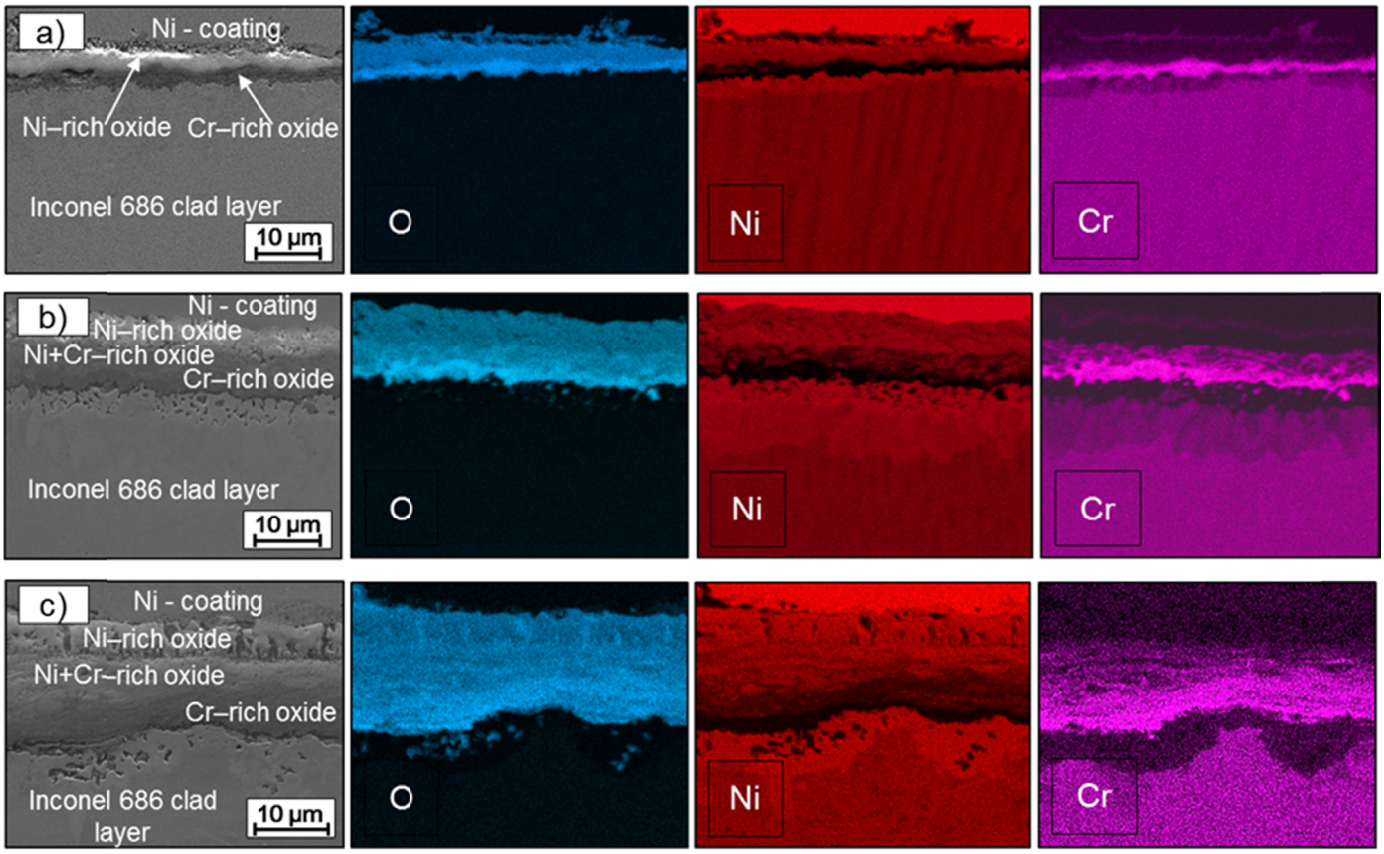

Fig. 6. SEM-EDS chemical composition mapping of a cross-section of Inconel 686 clad layer after exposure at 650°C in ashes for: a) 100 h; b) 1000 h and c) 2000 h showing the oxide scale

and combination with oxygen. Nickel oxide is not as stable as Cr_2O_3 or Cr_2NiO_4 [30].

Due to the 23% Cr-content in the weld clad, developed Cr_2O_3 scale is continuous, what is in agreement with literature data. The minimum concentration of chromium, needed for the formation of a passive Cr_2O_3 oxide film ranges from 20 to 25% [30].

Oxide scale growth resulting with distinct nickel and chromium depleted region present in the clad layer. It is characterized by high porosity and impacts on the composition of the clad, especially in the near-surface area where the concentration of nickel is significantly higher than in the deeper part of material. The chemical composition of the Inconel 686 clad layer becomes heterogeneous. The presence of the Cr-depleted zone due to the outward diffusion is confirmed by numerous studies [23,31,32]. In the innermost layer of oxide scale, the Cr content is considerably enhanced, on the average, by 75% relative to the Cr content in clad layer core, what confirms the formation of chromium oxide there. SEM-EDS chemical composition analysis (Fig. 6) showed that the chromium depleted zone was developed beneath oxide scale. It is consequence of selective oxidation of Cr to the Cr_2O_3 and Cr_2NiO_4. Cr-depleted zone is deeper after a longer time of oxidation, therefore strong enrichment in Ni was noticed. Occurrence of the Ni-enriched region results from the creation of the passive Cr_2O_3 layer on the surface of the Inconel 686 alloy, which significantly reduced diffusion of nickel into oxide scale.

3. Conclusions

During cladding boiler elements with nickel alloys, like Inconel 686, it is necessary to choose the best cladding technique to minimize the iron content in the clad layer (lower than 7% for inner and less than 2% in outer region of coating). The CMT technique is recommended for cladding boiler components for waste incineration power plants. The corrosion processes of the clad layer occurring under the impact of ashes from waste incineration plants, induce the formation of 1-2 µm thick Cr_2O_3 oxide layer in the innermost part of oxide scale after 100 h, which constitutes a passivation layer. Coarse grained NiO is formed in outermost region. Cr_2NiO_4 is formed between Cr_2O_3 and NiO. Right beneath outermost region, regions enriched alternately with NiO and Cr_2NiO_4 are present. A $CrNi_2O_4$ spinel is grown between NiO and Cr_2NiO_4. Cr_2O_3 passive layer protects the Inconel 686 clad layer from further degradation in aggressive environments, mainly by reduction of the diffusion rate of nickel towards the oxide scale.

Acknowledgments

The project was financed by National Science Centre, Poland. Grant number DEC-2014/15/N/ST8/02625.

REFERENCES

[1] Special Metals Corporation, www.Specialmetals.com, Corrosion-Resistant Alloys.

[2] R. Zhang, S.D. Kiser, B.A. Baker, Nickel alloy weld overlays improves the life of power generation boiler tubing, Special metals welding products company (2007).

[3] J.N. Dupont, S. Babu, S. Liu, Welding of materials for energy applications, Metall. Mater. Trans. A. **44**, 3385-3410 (2013). DOI: https://doi.org/10.1007/s11661-013-1643-9

[4] C. T. Sims, A contemporary view of nickel-base superalloys, JOM. **18**, 1119-1130, (1966). DOI: https://doi.org/10.1007/BF03378505

[5] S. Mrowec, T. Werber, Gas corrosion of metals, National Centre for Scientific, Warsaw, 1978.

[6] K.P. Lillerud, P. Kofstad, Sulfate-induced hot corrosion of nickel, Oxid. Met. **21**, 233-270 (1984). DOI: https://doi.org/10.1007/BF00656835

[7] U.K. Chatterjee, S.K. Bose, S.K. Roy, Environmental degradation of metals: Corrosion technology series/14, CRC Press, ISBN 9780824799205, 2001.

[8] Z. Zeng, K. Natesan, Z. Cai, D.L. Rink, Effect of coal ash on the performance of alloys in simulated oxy-fuel environments, Fuel. **117**, 133-145 (2014). DOI: https://doi.org/10.1016/j.fuel.2013.09.021

[9] Y. Niu, H. Tan, Ash-related issues during biomass combustion : Alkali-induced slagging, silicate melt-induced slagging (ash fusion), agglomeration , corrosion , ash utilization, and related countermeasures, Prog. Energy Combust. Sci. **52**, 1-61 (2016). DOI: https://doi.org/10.1016/j.pecs.2015.09.003

[10] D.L. Douglass, The oxidation mechanism of dilute Ni-Cr alloys, Corros. Sci. **8**, 665-678 (1968).

[11] D.J. Young, High Temperature Oxidation and Corrosion of Metals: Second Edition, Elsevier, New York, 2016.

[12] T. Tsao, A. Yeh, J. Yeh, M. Chiou, C. Kuo, H. Murakami, K. Kakehi, High temperature properties of advanced directionally – solidified high entropy superalloys, Superalloys 2016 13th Int. Symp. 1001-1009 (2016). DOI: https://doi.org/10.3390/e18020062

[13] K. Fueki, J.B. Wagner, Studies of the oxidation of nickel in the temperature range of 900 to 1400, J. Electrochem. Soc. **112**, 384-388 (1965).

[14] W.C. Hagel, A.U. Seybolt, Cation diffusion in Cr2O3, J. Electrochem. Soc. 1146-1152 (1961).

[15] K.H. Chang, J.H. Huang, C. Bin Yan, T.K. Yeh, F.R. Chen, J.J. Kai, Corrosion behavior of Alloy 625 in supercritical water environments, Prog. Nucl. Energy. **57**, 20-31 (2012). DOI: https://doi.org/10.1016/j.pnucene.2011.12.015

[16] C. Wagner, Formation of composite scales consisting of oxides of different metals, J. Electrochemi. Soc. **103**, 627-633 (1956).

[17] C.G. Pickin, S.W. Williams, M. Lunt, Characterisation of the cold metal transfer (CMT) process and its application for low dilution cladding, J. Mater. Process. Technol. **211**, 496-502 (2011).

[18] J. Adamiec, High temperature corrosion of power boiler components cladded with nickel alloys, Mater. Charact. **60**, 1093-1099 (2009). DOI: https://doi.org/10.1016/j.matchar.2009.03.017

[19] J. Słania, R. Krawczyk, S. Wójcik, Quality requirements put on the Inconel 625 austenite layer used on the sheet pile walls of the boiler's evaporator to utilize waste thermally, Arch. Metall. Mater. **60**, 677-685 (2015). DOI: https://doi.org/10.1515/amm-2015-0192

[20] M. Solecka, J. Kusiński, A. Kopia, M. Rozmus-Górnikowska, A. Radziszewska, High-temperature corrosion of Ni-base alloys by waste incineration ashes, Acta Phys. Pol. A. **130** (2016). DOI: https://doi.org/10.12693/APhysPolA.130.1045

[21] M. Solecka, A. Kopia, A. Radziszewska, B. Rutkowski, Microstructure, microsegregation and nanohardness of CMT clad layers of Ni-base alloy on 16Mo3 steel, J. Alloys Compd. **751**, 86-95 (2018). DOI: https://doi.org/10.1016/j.jallcom.2018.04.102

[22] M. Solecka, A. Kopia, P. Petrzak, A. Radziszewska, Microstructure, chemical and phase composition of clad layers of Inconel 625 and Inconel 686, Arch. Metall. Mater. **63**, 513-518 (2018). DOI: https://doi.org/10.24425/118969

[23] M. Solecka, A. Radziszewska, B. Rutkowski, New insight on study of Ni-base alloy clad layer after oxidation at 650°C, Corros. Sci. **149**, 244-248 (2019). DOI: https://doi.org/10.1016/j.corsci.2019.01.013

[24] C.C. Silva, C.R.M. Afonso, A.J. Ramirez, M.F. Motta, H.C. Miranda, J.P. Farias, Assessment of microstructure of alloy Inconel 686 dissimilar weld claddings, J. Alloys Compd. **684**, 628-642 (2016). DOI: https://doi.org/10.1016/j.jallcom.2016.05.231

[25] J. Dille, M.F. Motta, H.C. de Miranda, C.C. Silva, C.C. Silva, Electron detection modes comparison for quantification of secondary phases of Inconel 686 weld metal, Mater. Charact. **133**, 10-16 (2017). DOI: https://doi.org/10.1016/j.matchar.2017.09.014

[26] B. Arulmurugan, M. Manikandan, Development of welding technology for improving the metallurgical and mechanical properties of 21st century nickel based superalloy 686, Mater. Sci. Eng. A. **691**, 126-140 (2017). DOI: https://doi.org/10.1016/j.msea.2017.03.042

[27] Y. Chen, T. Tan, H. Chen, Oxidation companied by Scale Removal: Initial and Asymptotical Kinetics, J. Nucl. Sci. Technol. **7**, 662-667 (2008).

[28] J. Xiao, N. Prud, N. Li, V. Ji, Influence of humidity on high temperature oxidation of Inconel 600 alloy: Oxide layers and residual stress study, Appl. Surf. Sci. **284**, 446-452 (2013). DOI: https://doi.org/10.1016/j.apsusc.2013.07.117

[29] S. Chevalier, F. Desserrey, J.P. Larpin, Oxygen transport during the high temperature oxidation of pure nickel, Oxid. Met. **64**, 219-234 (2005). DOI: https://doi.org/10.1007/s11085-005-6560-x

[30] Y.C. Ma, X.J. Zhao, M. Gao, K. Liu, High-Temperature oxidation behavior of a Ni-Cr-W-Al alloy, J. Mater. Sci. Technol. **27**, 841-845 (2011). DOI: https://doi.org/10.1016/S1005-0302(11)60152-7

[31] E. Schmucker, C. Petitjean, L. Martinelli, P. Panteix, S. Ben, M. Vilasi, Oxidation of Ni-Cr alloy at intermediate oxygen pressures . I . Diffusion mechanisms through the oxide layer, Eval. Program Plann. **111**, 474-485 (2016). DOI: https://doi.org/10.1016/j.corsci.2016.05.025

[32] R. Halder, P. Sengupta, G. Abraham, C.P. Kaushik, G.K. Dey, Interaction of Alloy 693 with borosilicate glass at high temperature, Mater. Today Proc. **3**, 3025-3034 (2016). DOI: https://doi.org/10.1016/j.matpr.2016.09.017